Dynamic Trajectory Planning for Robotic Knot Tying

Bo Lu, Henry K. Chu, and Li Cheng

Department of Mechanical Engineering
The Hong Kong Polytechnic University
Hong Hum, Hong Kong
bo.lu@connect.polyu.hk, henry.chu@polyu.edu.hk, mmlcheng@polyu.edu.hk

Abstract— **Knot tying is an important component of surgery. When surgeons perform such operation via a tele-operated robotic system, the limited dexterity and field-of-view often poses technical challenges to the surgeons. In this paper, a new knot-tying method is proposed to enhance the quality of robotic knot-tying practice with low supervision. The trajectories of the instruments that can maintain the suture tension during the loop winding were formulated through the developed equations and MATLAB was employed to simulate the trajectory profiles. The grippers of the two instruments were then manipulated to grasp the suture and dynamically follow the pre-defined trajectories so that a suture knot can be constructed. Experiments were conducted and the results confirm that suture loops can be successfully winded around the instrument without suture slippage.**

Keywords—**Knot Tying; Loop Suturing; Minimally Invasive Surgery; Robotic Surgery; Trajectory Planning**

I. INTRODUCTION

Robots have a long history in assisting surgeons for various surgical operations. Back in 1985, a modified PUMA robot was already used to guide a needle in a patient for brain biopsy [1]. Later, robotic systems were also employed to perform surgical removal of gallbladder and cancerous tissues [2]. With advances in robotic and surgical technologies, the use of robotic systems to facilitate minimally invasive surgery (MIS) has received increasing interest in the past few decades as it has potential to revolutionize the traditional surgery. Minimally Invasive Surgery, also known as laparoscopic surgery, offers numerous advantages such as smaller incision wounds, reduced sense of pain, and faster recovery time, as compared to the open surgery. Through the assistance of a dexterous robotic surgical system, surgeons can improve their accuracy and stability in manipulating the medical instruments while eliminating hand tremor and involuntary movement. To date, da Vinci System is regarded as the most renowned surgical robotic system, performing over 200,000 surgical operations worldwide every year [3].

At the end of the surgical operation, sutures are often used to close up the wound. Tying a surgical knot is a very important component of the operation as a badly or improperly tied knot could lead to consequences such as wound inflammation and scar formation [4]. Although surgeons are experienced to tie high-quality knots, it may still be challenging for them when replicating their knot-tying skills through a tele-operated robotic system. Comparing to our human hands, typical robotic systems can offer limited flexibility and mobility to the attached medical instruments (grippers). Also, the restrictions of confined environment and the field-of-view make knot tying difficult to be performed. Hence, researchers are actively investigating different techniques, which can improve or simplify the knot tying practice.

Over the years, a number of research studies on knot tying have been conducted, including fixture-assisted, suture modeling and trajectory planning approaches. For fixture-assisted approach, the free ends of the suture can be tied automatically using a fixture integrated at end of the medical instrument [5], or through a four-piece fixture [6]. The use of fixtures to perform knot tying is quick and reliable, but it requires some modification to the existing instruments, which may not be suitable for all types of surgical operations. The research on suture modeling mainly focuses on simulating the motion of the suture for knot tying, where the suture can be modelled as a spline of linear springs [7, 8], a non-uniform spline [9], a finite segment model [10, 11], or a deformable linear object [12, 13]. In contrast, the trajectory planning approach focuses on the movements of the instruments to interact with the suture [14, 15]. For instance, Yamakawa *et al.* [16] proposed a dynamic approach where a knot can be tied with a single robot arm at high speed. Mayer *et al.* [17] examined the use of recurrent neural networks to learn knot tying from training trajectories. Van den Berg *et al.* [18] proposed an iterative learning approach to generate the trajectory for the robots. Chow *et al.* [19-21] considered using the position information of the instruments and the suture to generate the trajectories for the instruments to perform knot tying.

In this paper, we present a new trajectory-based method to enhance the efficiency and quality of knot tying after the surgery. Trajectories of the instruments are generated to manipulate the suture for closing the wound on an artificial skin. While the conventional instrument-tie technique [22] mainly uses one instrument to wind the suture loop over another stationary instrument, this method incorporates both instruments to dynamically tie the knot, thereby reducing the time required to complete the process. To prevent suture slippage, the required relative positions between the two instruments and the sutures are integrated in the trajectory planning in order to maintain the tension of the suture when making the loops. Details of the method are discussed and experiments are conducted to examine the performance of the proposed method.

II. METHODOLOGY ON SURGICAL KNOT TYING

A. Knot Tying Procedure

Figure 1 illustrates the schematic diagram of a typical environment for performing knot tying with the instrument-tie technique. The whole manipulations of suturing consist of threading the suture through the tissue, followed by suture grasping, suture looping, tail grasping, suture pulling and knot tying. To create a surgical knot, the suture, led by one instrument, needs to accomplish at least two circles around the other instrument.
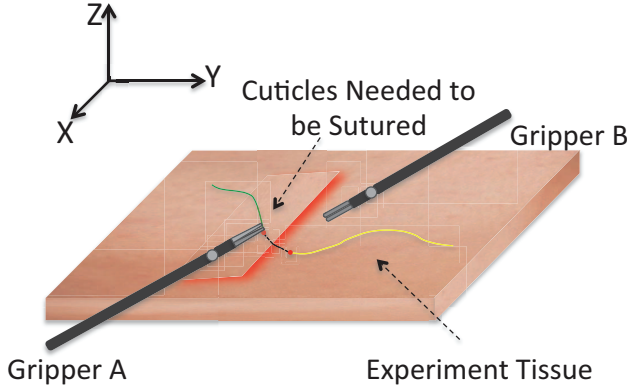

Figure 1. Schematic diagram of a typical surgical environment

The needle threading process refers to a puncture manipulation, in which the needle goes into the tissue at an entrance point and comes out from another exit point on the surface of the tissue as shown in Figure 2(a).

Similar to [19], the section between the needle exit point and the front point of the suture is defined as the leading segment (also the yellow suture in Figure 1), and the section between the needle entrance point and the end of this suture is defined as the suture's tail (also the green suture in Figure 1).
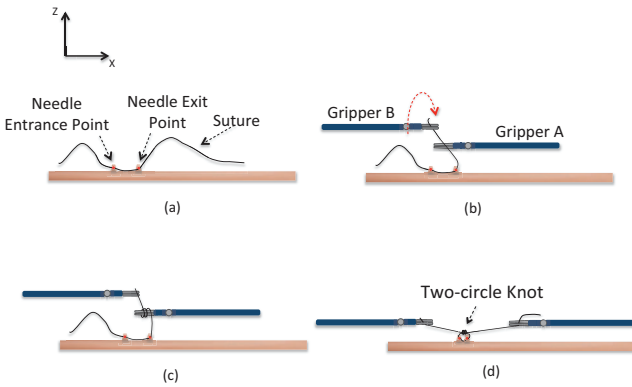

Figure 2. Front view (x-z plane) of the general suturing procedure

During the process of suture grasping, Gripper B needs to grasp the leading segment of the suture and Gripper A should be placed at a proper location in the workspace, which is shown in Figure 2(b). Then suture looping is followed, in which Gripper B should wrap the suture around Gripper A to form two circles, as illustrated in Figure 2(c). After completing the above procedures, tail grasping should come after. In this process, Gripper A moves slowly towards the tail of the suture, and grasps it. Then, these two grippers should be pulled in the opposite directions, and the tail of the suture goes through the two circles that constructed previously. Until this stage, a surgical knot is initially formed. Afterwards, the two grippers continue to move and tighten the knot. By pulling the suture to a proper degree of tightness, a standard surgical knot can be formed, which is shown in Figure 2(d). After completing the overall manipulations, the injured epidermis or wound can be sutured.

B. Trajectory Planning for Suture Looping

Suture looping is a relative standard process, but it could strongly affect the quality of the surgical knot. As discussed, the suture must be kept under tension when creating the loops and proper trajectory planning can be incorporated to achieve this objective. Figure 3 shows the side-view (*y-z* plane) of the suture looping process. After successful needle threading, Gripper A was positioned at a distance, *L*, from the needle exit point. To provide sufficient clearance for the process, Gripper A was kept at a minimum height of *H* above the tissue surface. Gripper B was manipulated to grasp the leading segment of the suture and positioned at a distance of *R* with respect to Gripper A, as shown in Figure 3(a).
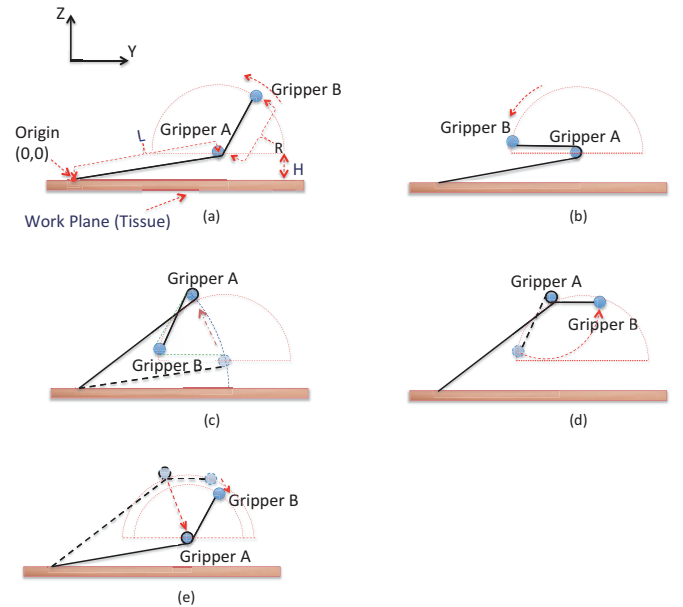

Figure 3. Side view (y-z plane) of the looping trajectory

In order to complete the first loop around Gripper A and also keep the length of the suture between two grippers at a constant value, Gripper B should move along a semi-round trajectory as shown in Figure 3(b). Then the movement of Gripper A should be followed. This operation is relatively

important among the whole manipulation process since slippage could easily occur. Ideally, the length of this suture between Gripper A and Gripper B, together with the length between Gripper A and the needle exit point should remain unchanged during the rotation. After this movement, Gripper B rotates around Gripper A and reaches the same height as Gripper A. Finally, Gripper A moves back to its original location, and simultaneously, Gripper B moves to a position, so that two grippers can form the same angle as the beginning.

Through the above trajectories, the first loop or circle of the surgical knot can be successfully constructed. By repeating the above procedures, the second loop can also be constructed to complete the suture looping. However, the above-mentioned scheme does not consider the dimensional effects of the two grippers. During the winding, the length of the suture can be reduced simultaneously, which can significantly affect the actual desired positions of the two grippers. Therefore, an additional parameter, r, which is the radius of the gripper, should be added when developing the trajectory equations.

As sketched in Figure 3(a), the needle exit point is denoted as the origin, and the initial angle between two grippers is set as θ. Therefore, the center coordinates of Gripper A and B can be expressed as:

$$\begin{cases} y_a^A = \sqrt{L^2 - H^2} \\ z_a^A = H \end{cases} \tag{1}$$

$$\begin{cases} y_a^B = \sqrt{L^2 - H^2} + R \cdot \cos\theta \\ z_a^B = H + R \cdot \sin\theta \end{cases} \tag{2}$$

where (y_a^A, y_a^A) and (z_a^B, y_a^B) are the coordinates of Gripper A and Gripper B respectively in Figure 3(a).

After the rotation, the length of the suture decreases as parts of the suture are wrapped around Gripper A, and the reduction is equal to the perimeter of a semi-circle. Hence, the coordinates of Gripper B should be:

$$\begin{cases} y_b^A = y_a^A \\ z_b^A = z_a^A \end{cases} \tag{3}$$

$$\begin{cases} y_b^B = \sqrt{L^2 - H^2} - R + \pi \cdot r \\ z_b^B = H + r \end{cases} \tag{4}$$

where (y_b^A, z_b^A) and (y_b^B, z_b^B) are the coordinates of Gripper A and Gripper B respectively in Figure 3(b).

After manipulating Gripper B to the position as shown in Figure 3(b), Gripper A should then rotate around Gripper B while maintaining a fixed distance so the suture should remain under tension. To better illustrate the procedure, the trajectory of Gripper A in Figure 3(c) is enlarged and shown in Figure 4.

The trajectory in the red dashed line is a circle arc, whose center is at Point A and the radius is equal to Line AB. Similarly, the trajectory in the blue dashed line is also an arc, which is the trajectory for the movement of Point B. It treats the origin as the center and the line between the origin and Point B as the radius.
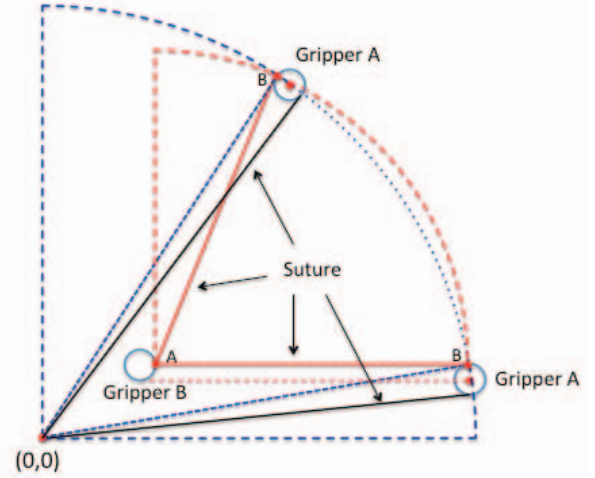

Figure 4. Detailed trajectory of Gripper A when rotating around Gripper B

Based on the schematic picture, the length between Point A and B can be evaluated as $R - (\pi + 1) \cdot r$ and the length between Point B and the origin can be evaluated as $\sqrt{[L^2 - H^2 + (H + r)^2]}$. Gripper A rotates with respect to the origin at an angle of α and the trajectory equation can be expressed as:

$$\begin{cases} y_c^{P\_B} = L1 \cdot \cos\alpha \\ z_c^{P\_B} = L1 \cdot \sin\alpha \end{cases} \tag{5}$$

$$L1 = \sqrt{[L^2 - H^2 + (H + r)^2]} \tag{6}$$

$$\begin{cases} y_c^A = y_c^{P\_B} + r \cdot \sin\alpha \\ z_c^A = z_c^{P\_B} - r \cdot \cos\alpha \end{cases} \tag{7}$$

$$\begin{cases} y_c^B = y_b^B \\ z_c^B = z_b^B \end{cases} \tag{8}$$

where $(y_c^{P\_B}, z_c^{P\_B})$, (y_c^A, z_c^A) and (y_c^B, z_c^B) are the coordinates of Point B on Gripper A, the center of Gripper A and the center of Gripper B in Figure 3(c), $L1$ represents the length of the suture between Point B and the origin.

In addition, the coordinates of Point B should satisfy the following equation:

$$\sqrt{(y_c^{P\_B} - y_c^B - r)^2 + (z_c^{P\_B} - z_c^B)^2} = R - (\pi + 1) \cdot r \tag{9}$$

In order to figure out $\left(y_c^{P\text{-}B}, z_c^{P\text{-}B}\right)$, MATLAB was used to simulate all points along the trajectory of Point B, and then, the corresponding coordinates (y_c^A, z_c^A) of Gripper A could be obtained.

After moving Gripper A to (y_c^A, z_c^A), Gripper B rotates around Gripper A to the same height. Considering the decrease of the suture length, the coordinates of two grippers can be represented as:

$$\begin{cases} y_d^A = y_c^A \\ z_d^A = z_c^A \end{cases} \tag{10}$$

$$\begin{cases} y_d^B = y_c^B + R - 2\pi r \\ z_d^B = z_c^B - r \end{cases} \tag{11}$$

where (y_d^A, z_d^A) and (y_d^B, z_d^B) are the coordinates of Gripper A and B in Figure 3(d).

Afterwards, Gripper A should move back to the original position, and simultaneously Gripper B moves to a new location:

$$\begin{cases} y_e^A = y_a^A \\ z_e^A = z_a^A \end{cases} \tag{12}$$

$$\begin{cases} y_e^B = y_a^A + (R - 2\pi r) \cdot \cos\theta \\ z_e^B = z_a^A + (R - 2\pi r) \cdot \sin\theta \end{cases} \tag{13}$$

where (y_e^A, z_e^A) and (y_e^B, z_e^B) are the coordinates of Gripper A and B in Figure 3(e).

As shown in Figure 3(e), after the first loop, two grippers move back to their original positions, only the length between them was shortened to $R - 2\pi r$. The suture looping process continued on to wind the second loop using the above procedures.

III. EXPERIMENT

A. Parameter Selection

To facilitate loop suturing, the leading segment of the suture must be sufficient to complete at least two loops. Otherwise, collision between the two grippers could occur while wrapping around the gripper. The gripper has a radius of 1.4mm and the minimum, R, must satisfy:

$$R - 4\pi r > 2r \tag{14}$$

The R value is calculated to be 21mm and other parameters used for the experiment, such as the length of the suture L between the needle exit point and Gripper A, the length of the segment R between two grippers and the value of the operating height H, are summarized in Table I.

TABLE I. PARAMETERS OF THE EXPERIMENT

Parameter	Value
L	21mm
H	4mm
θ	75°

As mentioned in the previous section, it is desirable to keep the suture length between Point A and Point B, and that between Point B and the origin, unchanged throughout the entire process. However, when rotating Gripper A with respect to the origin as shown in Figure 3(c), the section of the suture between Point A and B might be loosen. By employing MATLAB, the errors between the actual length and desired length between Point A and Point B can be simulated at different rotating angles α, and the results are summarized in Figure 5.
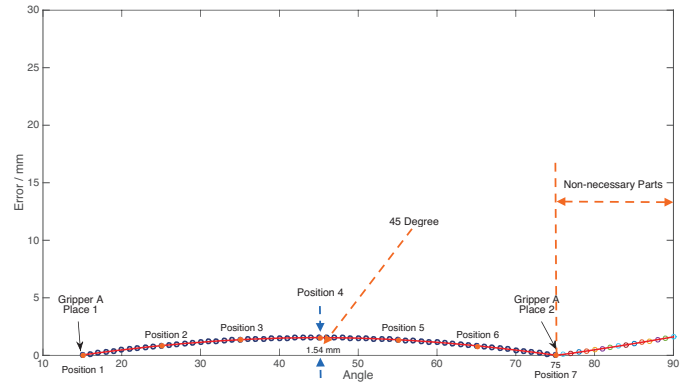

Figure 5. Errors between the true length and desired length of the section between Point A and Point B at different rotating angles

From the figure, the maximum error can be noticed, which is about 1.54mm at the rotating angle of 45 degree. Since the error is less than the half-perimeter of the gripper, therefore, the possibility of suture slippage can be negligible.
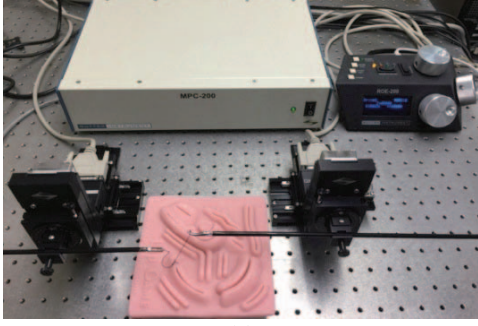
B. Experimental Setup

To simulate this surgical operation, an artificial tissue with a small cut was chosen to mimic the wound of a patient. Two laparoscopic graspers were employed to manipulate the suture for knot tying. The suture was made of non-absorbable synthetic polymer with a diameter of 0.2mm and 75cm long. The graspers were attached firmly to two independent motorized micromanipulators, MP-285, manufactured by Sutter Instruments.

In order to achieve this goal, the above-mentioned 3-DOF manipulators MP-285 can be appropriate. Each manipulator can provide 25mm of travel distance at a resolution of at least 0.2 microns on three axes.

In addition, a laparoscope-training platform was also included, together with a high-resolution camera, which can be used for further real-time image capture and the automated

control. Detailed specifications of the micromanipulators can be referenced to the manual.

(a)
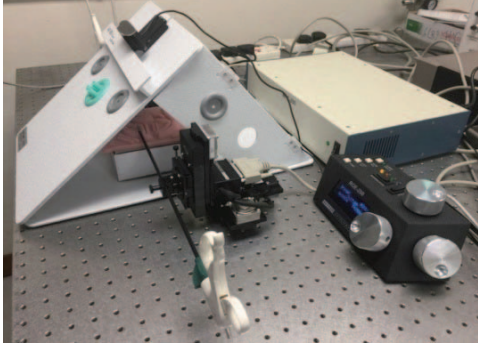
(b)

Figure 6. Experimental setup
(a). Robotic system without the cover of laparoscope operating platform;
(b). The system with the laparoscope operating platform

C. Experimental Result

The trajectory equations in Section IIB were implemented through the robotic system to examine the performance in completing loop suturing. MATLAB was used to simulate the trajectories of the two grippers in the first loop and their trajectory profiles are shown in Figure 7.
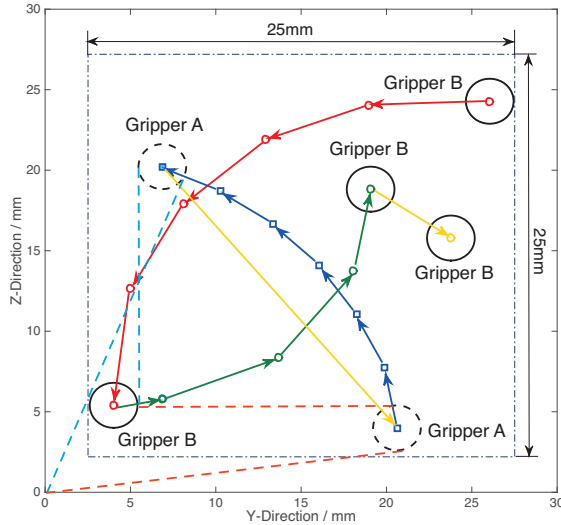

Figure 7. Trajectories of two grippers in the first loop

To simplify the control practice, the trajectories were discretized into 17 positions as tabulated in Table II and their

coordinates were sent to the micromanipulators of the system. Positions T1, T6, T12, T16 and T17 correspond to the locations of two grippers in Figures 3(a), (b), (c), (d) and (e), respectively. By dynamically manipulating the two grippers for loop winding, a workspace of $25mm \times 25mm$ is sufficient as we measured in Figure 7, offering a new approach for knot tying in a confined environment.
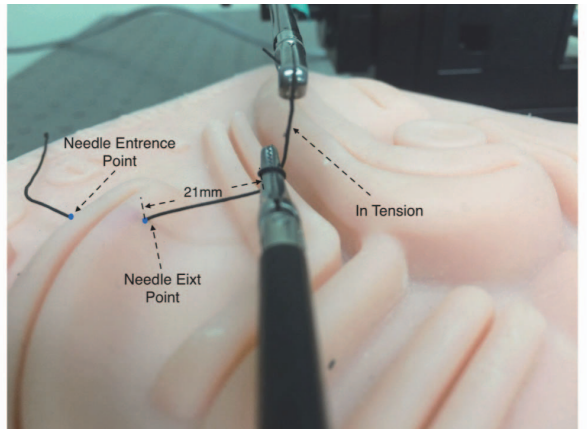
Completing the numerical simulations in MATLAB, the experimental validations of the proposed trajectories were followed. Figure8 (a) shows the initial state of the experiment. The two grippers were placed at the original locations respectively, with Gripper B grasping the leading segment of this suture.
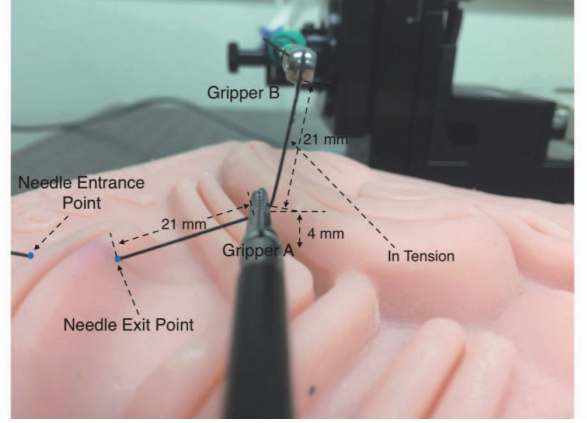
(a)
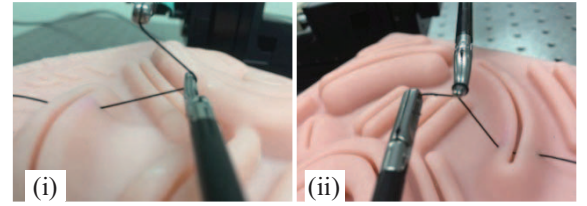
(b)

(c)

Figure 8. Experimental validations of the proposed trajectories

Afterwards, the procedures of the suture looping began. Figures 8(b)(i) and (ii) show the snap-shorts when the grippers are at T4 and T16 respectively. Following the calculated

coordinates of two grippers in Table II, a loop was successfully wrapped around Gripper A. As shown in Figure 8(c), after finishing the first loop of the winding, the length of the suture between Gripper A and the needle exit point was remained 21mm after the first loop. Besides, the leading segment between two grippers was also kept in tension. Repeating the above methods, the second loop of the surgical knot can also be accomplished. During the whole process, there was no slippgage or sliding, therefore, the proposed method can ensure the feasibility and the reliability for suture looping. Upon successful completion of this step, a high-quality surgical knot can be finished.

TABLE II.   Position Coordinates of the Grippers

TIME	Coordinates			
	Gripper A		Gripper B	
	Y / mm	Z / mm	Y / mm	Z / mm
T1	20.616	4.000	26.051	24.284
T2	20.616	4.000	18.988	24.008
T3	20.616	4.000	12.928	21.886
T4	20.616	4.000	8.099	17.917
T5	20.616	4.000	5.016	12.674
T6	20.616	4.000	4.014	5.400
T7	19.906	7.738	4.014	5.400
T8	18.260	11.077	4.014	5.400
T9	16.059	14.079	4.014	5.400
T10	13.370	16.654	4.014	5.400
T11	10.275	18.723	4.014	5.400
T12	6.868	20.223	4.014	5.400
T13	6.868	20.223	6.868	5.820
T14	6.868	20.223	13.703	8.384
T15	6.868	20.223	18.071	13.754
T16	6.868	20.223	19.072	18.823
T17	20.616	4.000	23.774	15.788

IV. Conclusion

In this paper, we have presented a new method to tie a surgical knot through a robotic surgical system. In contrast to the conventional instrument-tie technique, the two grippers of the system are both incorporated to perform the knot tying. One key advantage of the proposed method is to ensure the suture under tension during the entire looping process. To achieve this, the trajectories of the two grippers were formulated using the developed equations. Potential collisions between the two grippers were considered so that the loop suturing process can be performed with low supervision. The trajectories were simulated using MATLAB and examined experimentally. Results confirm that the suture loops can be constructed without suture slippage in a confined environment.

References

[1] A. R. Lanfranco, A. E. Castellanos, J. P. Desai, and W. C. Meyers, "Robotic Surgery: A Current Perspective," Ann Surg., 239(1), pp. 14–21, 2004.

[2] S. Breitenstein, A. Nocito, M. Puhan, U. Held, M. Weber, and P. A. Clavien, "Robotic-assisted versus laparoscopic cholecystectomy: outcome and cost analyses of a case-matched control study," Ann Surg., 247(6), pp. 987–993, 2008.

[3] N. Malhotra, P. Mittal, and R. Saxena, "Robotic Surgery," Operative Obstetrics and Gynecology, JP Medical Ltd, pp. 784, 2009.

[4] M. H. Kudur, S. B. Pai, H. Sripathi, and S. Prabhu, "Sutures and suturing techniques in skin closure," Indian J Dermatol Venereol Leprol, 75, pp. 425-434, 2009.

[5] T. Gopel, F. Hartl, A. Schneider, M. Buss, and H. Feussner, "Automation of suturing device for minimally invasive surgery," Surg. Endosc, 25, pp. 2100-2104, 2011.

[6] M. P. Ball, W. Wang, J. Kunzika, and D. Balkcom, "Knot-tying with four-piece fixtres," The International Journal of Robotics Research, 33(11), pp. 1481-1489, 2014.

[7] J. Philips, A. Ladd, and L. E. Kavraki, "Simulated Knot Tying," Proceedings of the IEEE International Conference on Robotics and Automation, pp. 841-846, 2012.

[8] H. F. Shi, and S. Payandeh, "Real-time Knotting and Unkotting," Proceedings of the IEEE International Conference on Robotics and Automation, pp. 2570-2575, 2007.

[9] N. Padoy, G. D. Hager, "3D thread tracking for robotic assistance in tele-surgery," Proceedings of the IEEE International Conference on Intellilgent Robots and Systems, pp. 2102-2107, 2011.

[10] J. Brown, J. Latombe, and K. Montgomery, "Real-time knot tying simulation," The Visual Computer, 20(2), pp. 165-179, 2004.

[11] H. Wang, S. Wang, J. Ding and H. Luo, "Suturing and tying knots assisted by a surgical robot system in laryngeal MIS," Robotica, 28, pp. 241-252, 2010.

[12] M. Saha, and P. Isto, "Manipulation Planning for Deformable Linear Objects," IEEE Transactions on Robotics, 23(6), pp. 1141-1150, 2007.

[13] H. Wakamatsu, A. Tsumaya, E. Arai, and S. Hirai, "Manipulation Planning for Knotting/Unknotting and Tightly Tying of Deformable Linaer Objects," Proceedings of the IEEE International Conference on Robotics and Automation, pp. 2505-2510, 2005.

[14] B. Ekci, "A simple technique for knot tying in single incision laparoscopic surgery (SILS)," Clinics, 65(10), pp. 1055-1057, 2010.

[15] S. Kudoh, T. Gomi, R. Katano, T. Tomizawa, and T. Suehiro, "In-air Knotting of Rope by a Dual-arm Multi-finger Robot," Proccedings of the IEEE International Conference on Intelligent Robots and Systems, pp. 6202-6207, 2015.

[16] Y. Yamakwa, A. Namiki and M. Ishikawa, "Motion Planning for Dynamic Knotting of a Flexible Rope with a High-spped Robot Arm," Proccedings of the IEEE International Conference on Intelligent Robots and Systems, pp. 49-54, 2010.

[17] H. Mayer, F. Gomex, D. Wierstra, I. Nagy, A. Knoll, and J. Schmidhuber, "A system for robotic heart surgery that learns to tie knots using recurrent neural networks," Proceedings of the IEEE International Conference on Intelligent Robots and Systems, pp. 543-548, 2006.

[18] J. van den Berg, S. Miller, D. Duckworth, H. Hu, A. Wan, X. Fu, K. Goldberg, and P. Abbeel, "Superhuman Performance of Surgical Tasks by Robots using Iternative Learning from Human-Guided Demonstrations," Proceedings of the IEEE International Conference on Robotics and Automation, pp. 2074-2081, 2010.

[19] D. Chow, and W. Newmann, "Improved Knot-tying methods for autonomous robot surgery," Proceedings of the IEEE Internatinal Conference on Autmation Science and Engineering, pp. 461-465,2013.

[20] D. Chow, R. C. Jackson, M. Cenk Cavusogluk and W. Newmann, "A novel vision guided knot-tying method for autonomous robotic surgery," Proceedings of the IEEE International Conferenec on Automation Science and Engineering, pp. 504-508, 2014.

[21] R. C. Jackson, R. Yuan, D. Chow, W. Newmann, and M. Cenk Cavusoglu, "Automatic initialization and dynamic tracking of surgical suture threads," Proceedings of IEEE International Conference on Robotics and Automation, pp. 4710-4716, 2015.

[22] R. F. Edlich, and W. B. Long, Surgical Knot Tying Manual, Third Edition, Covidien, pp. 78.